

Masses of Black Holes in Active Galactic Nuclei

Bradley M. Peterson*

Department of Astronomy and Center for Cosmology and Astro-Particle Physics, The Ohio State University

E-mail: peterson.12@osu.edu

Catherine J. Grier

Department of Astronomy, The Ohio State University

E-mail: grier.22@osu.edu

The masses of the central black holes have been measured for nearly 50 AGNs by using emission-line reverberation mapping. We briefly outline the process by which this is done and discuss the evidence about how reliable the derived masses might be. We outline how reverberation mapping underpins the mass estimates for all AGNs, including high-redshift quasars, and point out that the mass estimates are based on reasonable, yet unproven, assumptions. Finally, we briefly discuss results on reverberation velocity-delay maps that are revealing the kinematics of the broad-line region and yielding direct measurements of black hole masses.

Nuclei of Seyfert Galaxies and QSOs — Central Engine and Conditions of Star Formation

November 6-8, 2012

Max-Planck-Institut für Radioastronomie (MPIfR), Bonn, Germany

*Speaker.

1. Introduction

The two most important parameters in determining the physical characteristics of an active galactic nucleus (AGN) are the mass of the central black hole and the mass accretion rate — the rest is, arguably “engineering,” borrowing a description from Roger Blandford [5]. The demographics of black holes tells us about the accretion history of the universe [24] and, it is widely believed, something about the co-evolution of galaxies and black holes [9, 11]. Consequently, considerable efforts have been undertaken to measure the masses of central black holes in both active and quiescent galactic nuclei. Direct mass measurements, i.e., those based on observations of the acceleration of gas or stars by the black hole, generally involve modeling stellar or gas dynamics on resolvable angular scales or, in rarer cases, proper motion and radial velocities of megamasers or, in the singular case of our own Galaxy, individual stars. In each case, it is necessary to resolve (or nearly resolve) the black hole radius of influence, $R_{\text{BH}} = GM_{\text{BH}}/\sigma_*^2$, the region of the galactic nucleus where the stellar dynamics, characterized by the stellar velocity dispersion σ_* , are dominated by the black hole. Even with adaptive optics from the ground or with *Hubble Space Telescope*, the number of galaxies where R_{BH} is resolved is very limited and the number of *active* galaxies where R_{BH} is resolved is restricted to a bare handful.

Fortunately, in the case of AGNs, we can employ the alternative technique of “reverberation mapping,” [6, 21] which allows not only direct measurement of the black hole mass M_{BH} , but also reveals the nature of the gas flows in the immediate vicinity of the black hole. Reverberation mapping makes use of the fact that the continuum radiation from the accretion disk shows temporal variability of an irregular nature and the emission line-emitting gas responds to these variations with a time delay, or lag, that is attributed to the light-travel time across the broad-line region (BLR). By tracking these variations carefully (Figure 1), we can determine the structure and kinematics of the BLR. Reverberation mapping, in essence, substitutes time resolution for spatial resolution.

2. Reverberation-Based Masses

Assuming that the dynamics of the BLR gas are dominated by the gravity of the black hole, a virial estimate of the black hole mass requires only a characteristic size estimate for the BLR and a characteristic velocity dispersion. The size of the BLR is determined by measuring the time delay τ between continuum and emission-line flux variations (see [28] for the most up-to-date methodology) and inferring from this the size of the BLR $R = c\tau$. The velocity dispersion ΔV of the BLR gas is obtained directly from the emission-line width, although there is no consensus on the optimal way to characterize the line width¹. The black hole mass is then

$$M_{\text{BH}} = f \left(\frac{\Delta V^2 R}{G} \right). \quad (2.1)$$

The quantity in parentheses is the “virial product,” based on the two observable quantities, BLR radius and emission-line width, and has units of mass. The dimensionless factor f depends on

¹We have argued elsewhere [22] that the best characterization of the emission-line width is the line dispersion, or second moment, of the emission line in the rms residual spectrum formed from the many spectra obtained in the reverberation monitoring campaign. Use of FWHM seems to introduce biases that are a function of accretion rate. Widths of best-fit Gaussians do the same.

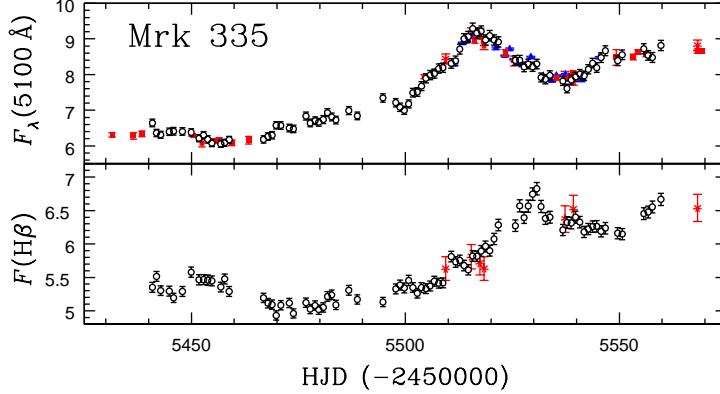


Figure 1: Mrk 335 continuum (top) and broad $H\beta$ emission-line light curves.[14]

the structure, velocity field, and inclination of the BLR and is thus different for each AGN; all the factors that we cannot determine from the simple prescription above are subsumed into f , which thus remains indeterminant. However, if we have another measure of the black hole mass for some number of AGNs, we can at least compute an ensemble average value. Since the relationship between central black hole mass and host galaxy bulge velocity dispersion (the “ $M_{\text{BH}}-\sigma_*$ relation”) observed for quiescent galaxies [9, 11] also seems to hold for active galaxies [10, 12], it has been used to establish a mean value of $\langle f \rangle \sim 5$ [19, 27]; moreover, the dispersion around this relationship (~ 0.4 dex) suggests that the intrinsic scatter in f is not extremely large. We must note, however, that it has been argued that this approach is oversimplified [13] and that the possible importance of radiation pressure has been neglected [18]. In any case, this empirical value for $\langle f \rangle$ is almost certainly good to within a factor of 2–3.

How reliable are reverberation-based masses from this prescription? At the level of 0.3–0.4 dex, they probably are reasonably good, certainly for measurements based on the Balmer lines. In addition to the general consistency with the $M_{\text{BH}}-\sigma_*$ relation, the veracity of these mass estimates is supported by other lines of evidence:

1. The time lag for each emission line in a given AGN is different, with the higher-ionization lines responding faster than the low-ionization lines. The high-ionization lines are broader as well, such that the virial product is constant for each emission line ([23, 1] and references therein).
2. Adopting the $M_{\text{BH}}-\sigma_*$ calibration of the reverberation mass scale, we find that there is also good consistency with the relationship between central black hole mass and host galaxy bulge luminosity [3].
3. In a few cases where black hole masses can be measured by using other techniques, to within the stated uncertainties, the reverberation-based masses are in generally good agreement with those based on other techniques (Table 1).

Table 1: Black Hole Masses (Units of $10^6 M_\odot$; see [22] for references)

Galaxy		NGC 3227	NGC 4151
<i>Direct methods:</i>	Stellar dynamics	7–20	< 70
	Gas dynamics	20^{+10}_{-4}	$30^{+7.5}_{-22}$
	Reverberation	7.63 ± 1.7	46 ± 5
<i>Indirect methods:</i>	$M_{\text{BH}}-\sigma_*$	25	6.1
	$R-L$ scaling	15	65

3. Indirect Mass Measurements Based on Reverberation

One of the most important, though anticipated, results of reverberation studies has been characterization of the relationship between AGN luminosity and BLR radius (the “ $R-L$ relation”). The slope of the relation, $R \propto L^{1/2}$ [2], is consistent with the most naïve expectations from photoionization theory. A great deal of the importance of this relationship derives from the fact that the AGN luminosity can be used to infer the BLR radius, and thus equation (2.1) can be applied based on only a single spectrum of an AGN, as was done in the bottom entry in Table 1.

While this is quite a simple idea, there are open issues regarding practical use of the $R-L$ relation with equation (2.1), which include the following:

1. The $R-L$ relation is empirically well-characterized only for the $\text{H}\beta$ emission line. There is evidence that a similar $R-L$ relation holds for $\text{C IV } \lambda 1549$, although this is based on a very small number of measurements [17].
2. There are a several potential difficulties in characterizing the BLR velocity dispersion, including what line-width measure is most appropriate, and how the line-width measurements are affected by blending with other features (emission and absorption) and the presence of non-variable components [8].

4. Velocity–Delay Maps

Determining black hole masses as described in §2 does not make use of all the information inherently available in reverberation data. Additional information can be extracted by measuring the emission-line response as a function of line-of-sight velocity (Doppler shift). The observed emission-line flux variations as a function of ΔV and time can be written as

$$L(\Delta V, t) = \int \Psi(\Delta V, \tau') C(t - \tau') d\tau', \quad (4.1)$$

where $C(t)$ is the continuum light curve, $L(\Delta V, t)$ is the velocity-resolved emission-line light curve, and $\Psi(\Delta V, \tau)$ is the “velocity–delay map.” It can be seen by inspection that the velocity–delay map is the observed response of the emission-line to a delta-function continuum outburst. By careful spectrophotometric monitoring of an AGN over time, it should be possible to recover the velocity–delay map from the observed continuum and emission-line light curves. This is actually very technically demanding [16] as the intrinsic levels of continuum and emission-line variability are

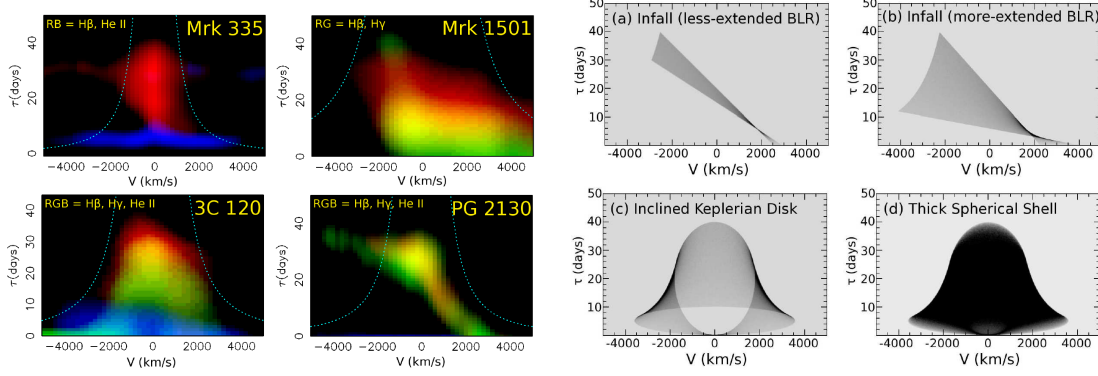


Figure 2: Left: Velocity–delay maps for 4 AGNs. Right: Toy models of velocity–delay maps for spherical infall (top two panels) and a Keplerian disk (lower left) and a thick shell of randomly inclined circular Keplerian orbits (lower right). [15].

generally not very large, typically $\sim 10\text{--}20\%$ (rms) over a few times the reverberation timescale. Some early attempts to recover velocity–delay maps hinted at interesting structure [25, 26], but it is only recently that high-fidelity velocity–delay maps have begun to appear [4, 15]. Examples are shown in the left half of Figure 2. While detailed physical modeling remains to be done in order to understand all the information in each of these maps, the “toy models” in the right half of Figure 2 provide us with some insight. Some velocity–delay maps strongly hint at a disk-like geometry (e.g., 3C 120). And while it is always dangerous to draw sweeping conclusions from a bare handful of objects, we nevertheless note that in each case observed to date the Balmer lines *always* show evidence for infall (i.e., the response from the near-side of the BLR, with smaller time delays is redshifted, and the response from the far side, with larger time delays, is blueshifted). It would be particularly interesting to obtain velocity–delay maps for C IV $\lambda 1549$ for these same systems, as there is abundant evidence that the higher-ionization UV resonance lines arise in material that is in *outflow*.

Velocity-resolved reverberation data can be modeled to determine the kinematics and structure of the BLR and, of course, derive the black hole mass directly. At this time, such modeling has been undertaken for only two sources, Arp 151 (a.k.a. Mrk 40) [7] and Mrk 50 [20] and in both cases, the masses derived are reassuringly consistent with those based the simple prescription of §2.

Acknowledgments

The authors are grateful for support of this research at The Ohio State University by the NSF through grant AST-1008882 and by NASA through grants HST-GO-11661 and HST-AR-12149 from the Space Telescope Science Institute. CJG gratefully acknowledges support from an Ohio State University Presidential Fellowship. The authors apologize for the limited reference list necessitated by space considerations.

References

- [1] M.C. Bentz *et al.* 2008, *ApJ*, **689**, L21–L24.
- [2] M. C. Bentz, B. M. Peterson, H. Netzer, R. W. Pogge, & M. Vestergaard 2009, *ApJ*, **697**, 160–181.
- [3] M. C. Bentz, B. M. Peterson, R. W. Pogge, & M. Vestergaard 2009, *ApJ*, **694**, L166–L170.
- [4] M.C. Bentz *et al.* 2010, *ApJ*, **720**, L46–L51.
- [5] R.D. Blandford in *Probing the Physics of Active Galactic Nuclei by Multiwavelength Monitoring*, ed. B.M. Peterson, R.S. Polidan, & R.W. Pogge, ASP Conference Series Vol. 224, (San Francisco: Astronomical Society of the Pacific), p. 499
- [6] R. D. Blandford & C. F. McKee 1982, *ApJ*, **255**, 419–439.
- [7] B. J. Brewer *et al.* 2011, *ApJ*, **733**:L33.
- [8] K. D. Denney 2012, *ApJ*, **759**:44.
- [9] L. Ferrarese & D. Merritt 2000, *ApJ*, **539**, L9–L12.
- [10] L. Ferrarese, R. W. Pogge, B. M. Peterson, D. Merritt, A. Wandel, & C. L. Joseph 2001, *ApJ*, **555**, L79–L82.
- [11] K. Gebhardt *et al.* 2000, *ApJ*, **539**, L13–L16.
- [12] K. Gebhardt *et al.* 2000, *ApJ*, **543**, L5–L8.
- [13] A. W. Graham, C. A. Onken, E. Athanassoula, & F. Combes 2011, *MNRAS*, **412**, 2211–2228.
- [14] C.J. Grier *et al.* 2012, *ApJ*, **755**:60.
- [15] C.J. Grier *et al.* 2013, *ApJ*, **764**:47.
- [16] K. Horne, B. M. Peterson, S. J. Collier, & H. Netzer 2004, *PASP*, **116**, 465–476.
- [17] S. Kaspi, W. N. Brandt, D. Maoz, H. Netzer, D. P. Schneider, & O. Shemmer 2007, *ApJ*, **659**, 997–1007.
- [18] A. Marconi, D. J. Axon, R. Maiolino, T. Nagao, G. Pastorini, P. Pietrini, A. Robinson, & G. Torricelli 2008, *ApJ*, **678**, 693–700.
- [19] C. A. Onken, L. Ferrarese, D. Merritt, B. M. Peterson, R. W. Pogge, M. Vestergaard, & A. Wandel 2004, *ApJ*, **615**, 645–651.
- [20] A. Pancoast *et al.* 2012, *ApJ*, **754**:49.
- [21] B. M. Peterson 1993, *PASP*, **105**, 247–268.
- [22] B. M. Peterson, in *Proceedings of the Workshop Narrow-Line Seyfert 1 Galaxies and Their Place in the Universe*, PoS (NLS1) 032.
- [23] B. M. Peterson *et al.* 2004, *ApJ*, **613**, 682–699.
- [24] A. Softan 1982, *MNRAS*, **200**, 115–122.
- [25] M.-H. Ulrich & K. Horne 1996, *MNRAS*, **283**, 748–758.
- [26] I. Wanders *et al.* 1997, *ApJ*, **453**, L87–L90.
- [27] J. Woo *et al.* 2010, *ApJ*, **716**, 269–280.
- [28] Y. Zu, C. S. Kochanek, & B. M. Peterson 2011, *ApJ*, **735**:80.